Indian J. Phys. 77A (5), 465–471 (2003)

AN INTERNATIONAL JOURNAL
IJPA

Microscopic study of low spin yrast levels in even-even krypton isotopes in the variation after projection approach

Tariq Ahmad War, Anil Chandan, Rani Devi, Arun Bharti and S K Khosa*

Department of Physics, Jammu University, Jammu-180 006, India

E-mail . tariqwar_war@yahoo co.in

Received 29 November 2002, accepted 19 June 2003

Abstract : Variation after projection (VAP) calculations in conjunction with Hartree-Bogoliubov (HB) ansatz have been carried out for A = 74–82 krypton isotopes In this framework, the yrast spectra with $J^{\pi} \leq 16^{+}$, $B(E2)$ transition probabilities, quadrupole (β_2) deformation parameter have been obtained The results of the calculation give an indication that it is important to include the hexadecapole-hexadecapole component of the two-body interaction for obtaining various nuclear structure quantities in Kr isotopes Besides this the yrast spectra in ^{76,78}Kr isotopes arise from two intrinsic states.

Keywords · Nuclear structure ^{72}Kr, variation-after-projection calculations, calculated levels, $B(E2)$ transition probabilities, quadrupole (β_2) deformation parameter.

PACS Nos. : 27 50 +e; 21 60.Jz, 21 10. Re, 23.20-g

1. Introduction

Recent years have witnessed a rapid increase in the experimental activity of measuring the properties of the yrast levels (with $J^{\pi} \leq 16^{+}$) as well as $E2$ transition [1–12] in krypton isotopes. The available experimental information in the nuclei ^{74,76,78}Kr suggest existence of sizeable quadrupole deformation and the associated rotational collectivity in the ground states. The (E_2^{+}–E_0^{+}) energies in these isotopes range between 0.42 MeV to 0.45 MeV and the $B(E2; 0_1^{+}–2_1^{+})$ values are more than $0.67e^2b^2$. The available information in the nuclei ^{80,82}Kr on the other hand, implies a significant reduction of rotational collectivity; the (E_2^{+}–E_0^{+}) values lie in the range 0.61 MeV to 0.77 MeV and the observed $B(E2; 0_1^{+}–2_1^{+})$ estimates are $0.41e^2b^2$ and $0.23e^2b^2$ respectively.

Sometime back, Praharaj [13] carried a deformed Hartree-Fock (HF) calculation for even–even krypton isotopes. His calculation revealed that $^{72-80}$Kr seem to be oblate in shape while for ^{82}Kr there is near degeneracy of oblate and prolate shapes. In a calculation for the shapes of Kr nuclei using a deformed Saxon-wood potential and the Struntisky shell procedure, Nazarewicz *et al* [14] found that ^{72}Kr is oblate, $^{74-76}$Kr are prolate and for ^{78}Kr, there is prolate-oblate degeneracy. In the calculation of Moller and Nix [15] in microscopic model using a finite–range nuclear force, it turns out that $^{70-72}$Kr is oblate, $^{74–76}$Kr are prolate, ^{78}Kr is oblate while ^{82}Kr have a small prolate deformation. Nuclei in this mass region have also been investigated by HF calculation using density dependent effective interaction of Skyrme type (Bonche *et al* [16]). In the calculation of Campi and Epherre [17] even mass krypton nuclei A = 74–92 have negligible deformations while for ^{94}Kr and higher masses there is a sudden onset of large prolate deformation. In the calculation of Bonche *et al* [16], ^{74}Kr and ^{76}Kr are prolate.

Apart from the above mentioned theoretical works, a large number of recent calculations have attempted a description of the low spin yrast levels in krypton isotopes

*Corresponding Author

in the framework of phenomenological models [18–25]. An oblate minimum in ^{78}Kr is predicted by the relativistic mean-field calculations by Maharana *et al* [18]. The structure of collective bands in ^{78}Kr is studied within the framework of the deformed configuration mixing shell model by Tripathy and Sahu [19] and the calculated levels are grouped into collective bands on the basis of the B(E2) values among them. At $J = 8^+$, a neutron-aligned band crosses the ground band and becomes yrast. Sarriguren *et al* [20] have studied the ground state properties of proton-rich isotopes of krypton by using a deformed self consistent HF + RPA (Random Phase Approximation) approach and finds that most of the isotopes present two minima corresponding to two different shapes. Microscopic results concerning the shape co-existence and shape transition have been obtained within the complex version of the Excited Vampir Variational approach by Petrovici *et al* [21]. A strong mixing of prolate and oblate deformed configuration could also explain the irregularties observed at low excitation energy. Giannatiempo *et al* [22] have carried out calculations in the framework of the interacting boson model and the positive parity bands observed in the $^{72-84}$Kr isotopes. The analysis includes states of spin up to the maximum allowed by the finite boson number and the symmetry character of these bands in the proton and neutron degrees of freedom has been investigated. Gross *et al* [23] have used the cranked Hartee-Fock Bogoliubov model with Woods-Saxon potential to study the ground state deformation and the evolution of shape of krypton isotopes. Palit *et al* [24] have studied yrast-band structure of proton rich, even-even mass-80 nuclei in the framework of projected shell model approach and these nuclei exhibit many phenomena that are quite unique to this mass region. Soundranayagam *et al* [25] have performed two–quasiparticle plus rotor model calculations for ^{80}Kr. These calculations have been carried out in restricted $2p$-$1f$-$1g$-valence space. It would be very interesting to see how the results change if a larger valence space is employed and a single calculational framework is applied to all the proton rich krypton isotopes. It was seen by Khosa and Sharma [26] that two–body effective interactions have a dominantly quadrupole–quadrupole character and the deformation producing tendency of neutron–proton (np) and like particle interactions depends upon the degeneracy of the underlying single particle valence space.

We have therefore, examined the available yrast spectra for krypton isotopes in the framework of variation after projection (VAP) technique in conjunction with the HB ansatz for the trial wave function resulting from the pairing plus quadrupole–quadrupole plus hexadecapole-hexadecapole interaction (PQH) operating in a large valence space.

2. Calculational details

2.1. The one and two body parts of the Hamiltonian

In our calculations, we have employed the valence space spanned by $3s_{1/2}$, $2p_{1/2}$, $2p_{3/2}$, $2d_{3/2}$, $2d_{5/2}$, $1f_{5/2}$, $1g_{7/2}$, $1g_{9/2}$ and $1h_{11/2}$ orbits for protons and neutrons under the assumption of $N = Z = 28$ sub-shell closure. The single particle energies we have taken are (in MeV). $(3s_{1/2}) = 9.90$, $(2p_{1/2}) = 1.08$, $(2p_{3/2}) = 0.0$, $(2d_{3/2}) = 11.40$, $(2d_{5/2}) = 8.90$, $(1f_{5/2}) = 0.78$ $(1g_{7/2}) = 11.90$, $(1g_{9/2}) = 3.50$ and $(1h_{11/2}) = 12.90$. The energy values of single particle orbits for $2p$-$1f$-$1g$ levels are the same as employed for ^{56}Ni core plus one nucleon. The energies of higher single particle valence orbits is the same as used by Vergados and Kuo [27] relative to $1g_{9/2}$ valence orbit.

The two body effective interaction that has been employed is of pairing-plus-quadrupole-quadrupole-plus-hexadecapole- hexadecapole (PQH) type. The parameters of pairing-plus-quadrupole-quadrupole (PQ) part of the two body interaction are also the same as used by Sharma *et al* [28]. The relative magnitudes of the parameters of the hexadecapole-hexadecapole parts of the two body interaction were calculated from a relation suggested by Bohr and Mottelson [29]. According to them the approximate magnitude of these coupling constants for isospin $T = 0$ is given by

$$\chi_\lambda = \frac{4\pi}{2\lambda+1}\frac{m\omega_0^2}{A<r^{2\lambda-2}} \quad \text{for } \lambda = 1, 2, 3, 4 \qquad (1)$$

and the parameters for the $T = 1$ case are approximately half the magnitude of their $T = 0$ counterparts. This relation was used to calculate the values of χ_{pp4} relative to χ_{pp2} by generating the wavefunction for krypton isotopes and then calculating the values of $\langle r^2\lambda^{-2}\rangle$ for $\lambda = 2$, 3 and 4.

The values for hexadecapole-hexadecapole part of the two body interaction turn out to be

$\chi_{pp4} (=\chi_{nn4}) = -0.00033$ MeV b^{-8} and $\chi_{pn4} = -0.00066$ MeV b^{-8}

2.2 Projection of states of good angular momentum from Axially-symmetric HB intrinsic states :

The procedure for obtaining the axially symmetric HB intrinsic states has been discussed in Ref. [30].

The axially-symmetric HFB (Hartree-Fock-Bogoliubov) states can be written as

$$|\phi_0> = \prod_{im} (U_i^m + V_i^m b_{im}^\dagger b_{i\bar{m}}^\dagger)| 0 > , \quad (2)$$

where the creation operators $b_{im}^\dagger$ can be expressed as

$$b_{im}^\dagger = \sum_j c_\mu^m a_{jm}^\dagger , \quad b_{i\bar{m}}^\dagger = \sum_j (-1)^{j+m} c_\mu^m a_{j-m}^\dagger . \quad (3)$$

Here, the creation operators $a_{jm}^\dagger$ create a particle in the orbit $|nljm>$ and c_μ^m are the expansion coefficients. The index j labels the single-particle state and the index i is employed to distinguish between the different deformed single-particle states with the same $<\hat{j}_z> = m$.

The states with good angular momenta J projected from the HB state $|\Phi_K>$ can be written as

$$\Psi_K^J > = P_{KK}^J |\Phi_K> = [(2J+1)/8\pi^2] \int D_{KK}^J(\Omega) R(\Omega) |\Phi_K> d\Omega \quad (4)$$

where $R(\Omega)$ and $D_{KK}^J(\Omega)$ are the rotation operators of the rotation matrix, respectively.

The energy of the state with the angular momentum is given as

$$E_J = <\Phi_0 | HP_{00}^J | \Phi_0> / <\Phi_0 | P_{00}^J | \Phi_0> = \frac{\int_0^\pi h(\theta) d_{00}^J(\theta) d(\cos\theta)}{\int_0^\pi n(\theta) d_{00}^J(\theta) d(\cos\theta)} . \quad (5)$$

Here, the overlap integrals $h(\theta)$ and $n(\theta)$ are given by

$$h(\theta) = n(\theta)\Big| \sum \varepsilon(\alpha)\rho_{\alpha\alpha} - (G/4) \sum S_\alpha [f(1+M(\theta))^{-1}]_{\alpha\alpha}^{\tau_3} \sum_{\beta\tau_3} S_\beta [(1+M(\theta))^{-1} F(\theta)]_{\beta\beta}^{\tau_3} - (1/2) \sum_{\tau_3\tau_3'\mu} (-1)^\mu \chi_{\tau_3\tau_3'} \sum_{\alpha\gamma} <\alpha|q_\mu^2| \gamma> \rho_{\alpha\gamma}^{\tau_3} \sum_{\beta\delta} <\beta|q_{-\mu}^2|\delta> \rho_{\delta\beta} \quad (6)$$

where

$$n(\theta) = \{ \det [1 + M(\theta)] \}^{1/2}, \quad (7)$$

$$F_{\alpha\beta}(\theta) = \sum_{m'_\alpha m'_\beta} d^{j_\alpha}_{m_\alpha m'_\alpha}(\theta) d^{j_\beta}_{m_\beta m'_\beta}(\theta) f_{j_\alpha m'_\alpha, j_\beta m'_\beta} \quad (8)$$

$$f_{\alpha\beta} = \sum_i C^{m_\alpha}_{j_\alpha l_\alpha} C^{m_\beta}_{j_\beta l_\beta} \left(\frac{v_i^{m_\alpha}}{u_i^{m_\alpha}} \right) \delta_{m_\alpha, -m_\beta} , \quad (9)$$

$M(\theta) = F(\theta) f$ and

$$\rho\alpha\beta(\theta) = \{M(\theta)/[1+M(\theta)]\}_{\beta\beta} \delta_{\beta\beta} \{[1+M(\theta)]^{-1}\}_{\beta\beta} . \quad (10)$$

The yrast energies are calculated as follows. Using the results of the HB calculations which are summarized in terms of the amplitudes (u_i^m, v_i^m) and the expansion coefficients c_μ^m, we first set up the (50×50) f-matrix in the present configuration space. Then, $F(\theta)$, $M(\theta)$, and $(1+M(\theta))^{-1}$ are computed for 20 Gaussian quadrature points in the range (0, $\pi/2$). Finally, the projected energies are calculated employing eqs. (5)-(10).

2.3. The variation-after angular-momentum projection (VAP) Method.

The VAP calculations have been carried out as follows. We first generated the self-consistent HB solutions, $\Phi(\beta)$, by carrying out the HB calculations with the Hamiltonian $(H-\beta Q_0^2)$, where 'β' is a parameter. The selection of the optimum intrinsic states, $\Phi_{opt}(\beta_J)$, is then made by finding out the minimum of the projected energy

$$E_J(\beta) = <\Phi_0(\beta)|HP_{00}^J| \Phi_0(\beta)>/<\Phi_0(\beta)|P_{00}^J|\Phi_0(\beta)> \quad (11)$$

as a function of β. In other words, the optimum intrinsic state for each yrast J satisfies the condition.

$$\partial/\partial\beta [<\Phi_0(\beta)|HP_{00}^J|\Phi_0(\beta)>/<\Phi_0(\beta)|P_{00}^J|\Phi_0(\beta)>]|_{\beta=\beta_J} = 0. \quad (12)$$

3. Results and discussion

3.1 Intrinsic states :

The calculated quadrupole moments of the optimum intrinsic states associated with the yrast levels in the

nuclei ^{74,76,78,80,82}Kr have been presented in Table 1. Discussing first the results for $<Q^2_0>$ moments of the optimum intrinsic states associated with the ground states, we notice that the $<Q^2_0>$ values in the nuclei ^{74,76}Kr are isotopes. It appears from these results that the yrast spectra in $^{76-82}$Kr isotopes has a dichotomic structure. The 0^+ and 2^+ states arising from an intrinsic state having smaller deformation .

Table 1. Quadrupole moments $<Q^2_0>_{HB}$ of intrinsic states associated with yrast levels in the nuclei $^{74-82}$Kr. Here, $<Q^2_0>_{max}$ gives maximum values of intrinsic quadrupole moment for each isotope. The maximum value of the intrinsic quadrupole moment $<Q^2_0>_{max}$ is obtained by calculating the intrinsic quadrupole moment of the nucleus from the HB wave function generated by putting the single particle energies of all the valence orbits equal to zero

Kr nuclei	J^π	0^+	2^+	4^+			10^+	12^+	14^+	16^+	$<Q^2_0>_m$
(A)											
74		56.62	56.62	56.62	56.62	56.62	56.62	64 26	64 26	64.26	95.72
76		52.97	52.97	63.96	63.96	63.96	63.96	63.96	63.96	63.96	100.91
78		50.00	50.00	61.00	61.00	61.00	61.00	61.00	61.00	61.00	103.66
80		45.95	45.95	63.89	63.89	63.89	63.89	63.89	63.89	63.89	107.22
82		42.00	42.00	62.04	62.04	62.04	62.04	62.04	62.04	62.04	110.61

52 percent and for ^{78}Kr it is 48 percent of their maximum possible values for the given valence space. The maximum value of the intrinsic quadrupole moment $<Q^2_0>_{max}$ is obtained by calculating the intrinsic quadrupole moment of the nucleus from the HB wave function generated by putting the single particle energies of all the valence orbits equal to zero. This ties in nicely with the observed deformation systematics of E_2^+ in these isotopes. It is noteworthy that the intrinsic quadrupole moments of ground states systematically decrease from its value of 56.62 units for ^{74}Kr to 42 units in ^{82}Kr. However, it is noticed that energy states with $J^\pi \geq 4^+$ belong to a different intrinsic state having larger quadrupole moments for $^{76-82}$Kr

3.2. Yrast levels :

In Figures 1 and 2, we have displayed the observed [1–4] as well as theoretical yrast spectra resulting from the VAP method. Keeping in view the possibility of a change in the position of the calculated 0_1^+ states because of its mixing with the co-existing 0^+ states of spherical origin, we have focussed only on a comparison of the calculated and observed spectra for $J^\pi \geq 2^+$. We have therefore aligned the calculated 2^+ states with the observed one. It is seen that VAP spectra in the nuclei $^{74-82}$Kr for the low lying states is in reasonably good agreement with the experiment. The VAP prescription is seen to yield small but significant improvement over the Projected-Hartree-Bogoliubov (PHB)

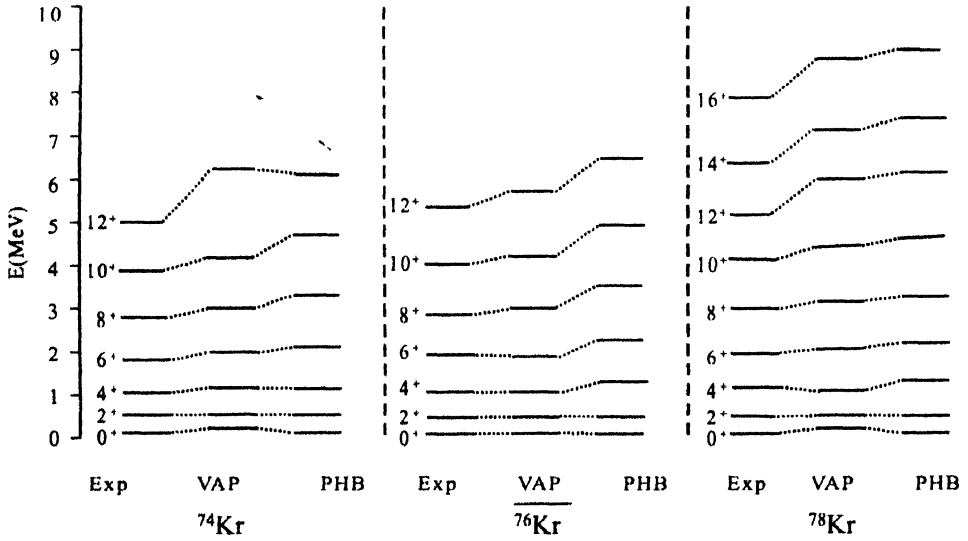

Figure 1. Experimental and theoretical low-lying yrast spectra for $^{74-78}$Kr nuclei Data taken from Refs. [1–3].

yrast energies in these nuclei. We find that the VAP energies for the yrast levels with $2^+ \leq J^\pi < 12^+$ in the nuclei $^{74\text{-}82}$Kr are in reasonable agreement with the observed ones. It is noted from our VAP calculation that the maximum deviation of our 10^+ state from the experimental

effects in krypton isotopes. We however, do not project out wavefunction of each angular momentum state and therefore can not quantitatively calculate the contribution to total angular momentum due to the $g_{9/2}$ nucleons.

3.3. B(E2) Transition probabilities :

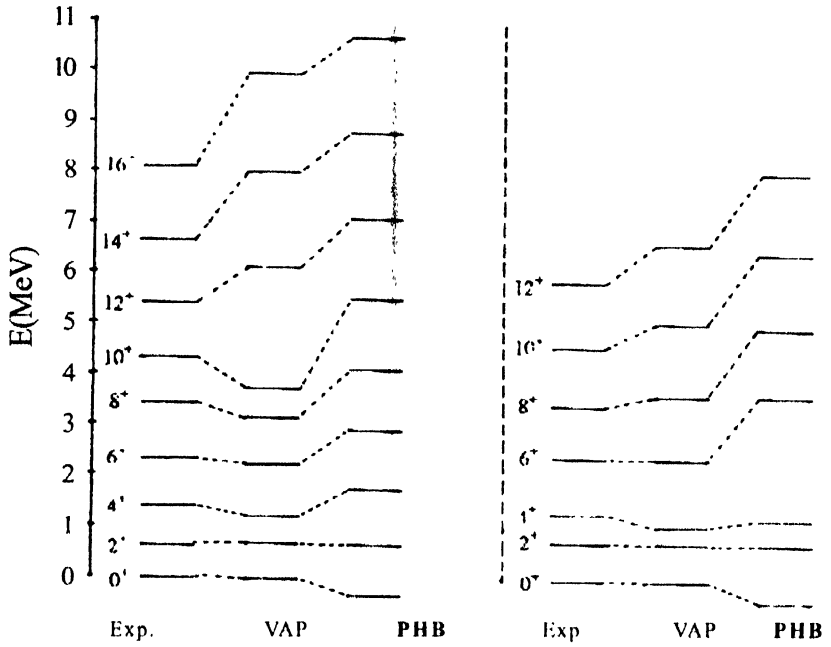

Figure 2. Experimental and theoretical low-lying yrast spectra for ^{80,82}Kr nuclei Data taken from Refs. [1,4].

value is about 0.6 MeV. Besides this, the compression of energy states observed in ^{80}Kr at 8^+ state and in ^{82}Kr at 6^+ state is reasonably well reproduced. The decrease in the observed energy spacing between 4^+ and 2^+ in $^{74\text{-}82}$Kr isotopes is due to the change of intrinsic state. On inspecting the HB wave function of the intrinsic state giving rise to angular momentum states with $J^\pi \leq 4^+$ in $^{76\text{-}82}$Kr, one observes the appearance of $g_{9/2,1/2}$ component in the protonic part of the wave function at the Fermi level. The neutron wave function however shows the appearance of $g_{9/2,3/2}$ component near the Fermi level for neutrons. It has been said by Praharaj [13] in his paper that such configuration which involves the occupation of large j and small m orbits are responsible for producing rotation alignment of nucleons which can in turn, produce sudden compression in energy levels. Since the intrinsic states that are producing energy levels with $J^\pi \geq 4^+$ have single particle HB orbits near the fermi energy having substantial occupation of $g_{9/2,1/2}$ and $g_{9/2,3/2}$ orbit components, it is likely to produce rotation alignment

The reliability and goodness of the HB wave function is examined by calculating the $B(E2; 0_1^+ \rightarrow 2_1^+)$ values. Bhatt *et al* [31,32] have developed formula for the calculation of $B(E2; 0_1^+ \rightarrow 2_1^+)$ transition probabilities from the values of intrinsic quadrupole moments of protons and neutrons. It has been justified by them that $B(E2; 0_1^+ \rightarrow 2_1^+)$ in units of $e^2 b^2$ are given by

$$B(E2; 0_1^+ \rightarrow 2_1^+) = (1.02 \times 10^{-5}) A^{2/3} c^2_{\text{model}} [e_\pi \langle Q^2_0 \rangle_\pi + e_\nu \langle Q^2_0 \rangle_\nu]^2. \quad (13)$$

where $\langle Q^2_0 \rangle_\pi$, ($\langle Q^2_0 \rangle_\nu$) are the intrinsic quadrupole moments of valence protons (neutrons) whereas $e\pi$ and $e\nu$ are the effective charges of the protons and neutrons, respectively. Effective charges of the protons and neutrons are 1.5 and 0.5, respectively for $^{74\text{-}82}$Kr isotopes. They have recommended the $c_{\text{model}} = (1.11 \pm 0.27)$ for $28 \leq Z \leq 50$ [33]. We have used this formula for the calculation of the $B(E2)$ values for the krypton isotopes.

In Table 2. we present a comparison of the calculated $B(E2)$ values obtained with PQH interaction with the

experimental values [5,6] for the $0_1^+ \rightarrow 2_1^+$ transitions in case of $^{74\text{-}82}$Kr. It is satisfactory to note that the calculated

Table 2. Comparison of the calculated and experimental $B(E2; 0_1^+ \rightarrow 2_1^+)$ values, quadrupole deformation parameter (β_2) of the HB states in $^{74\text{-}82}$Kr isotopes. $B(E2)$ values are in units of e^2b^2

Kr nuclei (A)	$B(E2; 0_1^+ \rightarrow 2_1^+)$		(β_2)	
	Th	Exp.	Th.	Exp.
74	0 84	0 89(8)*	0.38	0.387(40)**
76	0 57	0 79(6)*	0 37	(0 34)***
78	0 68	0 686(30)*	0.32	0.343(14)**
80	0 41	0 384(32)*	0 30	0 265(7)**
82	0 31	0 233(10)**	0 26	0 2022(45) **

* Data taken from Ref. [5]

**Data taken from Ref [6]

***Data taken from Ref. [7].

$B(E2)$ values are in satisfactory agreement with the experimental values for the $0_1^+ \rightarrow 2_1^+$ transitions in case of $^{74\text{-}82}$Kr. Since the calculations for the $B(E2)$ values depend on the intrinsic quadrupole moment, $B(E2)$ values should follow the same trend as that followed by the intrinsic quadrupole moments. This feature of the krypton isotopes has been reproduced by the present calculations.

3.4. Quadrupole (β_2) deformations :

In table 2, the calculated and experimental values for deformation parameter (β_2) have also been presented. The deformation parameter β_2 is related to $B(E2)\uparrow$ by the formula suggested by Raman *et al* [33].

$$\beta_2 = (4\pi/3ZR_0^2)\ [B(E2)\uparrow /e^2]^{1/2} \qquad (14)$$

where R_0 is usually taken to be $1.2A^{1/3}$ fm and $B(E2)\uparrow$ is in units of $e^2\ b^2$.

From the systematics of the calculated β_2 values, it is noted that the set of values obtained with PQH interaction are in satisfactory agreement with the observed values.

3.5 Occupation numbers for shell model orbits :

In Tables 3 and 4, we have given the results for the occupation numbers of the $3s_{1/2}$, $2p_{1/2}$, $2p_{3/2}$, $2d_{3/2}$, $2d_{5/2}$, $1f_{5/2}$, $1g_{7/2}$, $1g_{9/2}$ and $1h_{11/2}$ orbits for the various angular momentum states in $^{74\text{-}82}$Kr. The study of proton

Table 3 The sub-shell occupation numbers (protons) in the nuclei $^{74\text{-}82}$Kr

Kr nuclei (A)	Sub-shell occupation number								
	J^π	$3s_{1/2}$	$2p_{1/2}$	$2p_{3/2}$	$2d_{3/2}$	$2d_{5/2}$	$1f_{5/2}$	$1g_{7/2}$	$1g_{9/2}$	$1h_{11/2}$
74	0^+ 10^+	0 08	0.60	2.63	0.06	0.44	2 79	0 03	1 69	0 09
	12^+–16^+	0.13	0.52	2.09	0.09	0 57	2 67	0.05	1.88	–0 003
76	0^+–2^+	0.09	0.51	2.30	0.05	0.40	2 79	0.03	1.68	0 09
	4^+–16^+	0 16	0.52	1 95	0.11	0 64	2.41	0.07	2.00	0.10
78	0^+–2^+	0.09	0.51	2.32	0.05	0.40	2 76	0.03	1.68	0 11
	4^+ 16^+	0.15	0.51	2.01	0 10	0.61	2.49	0 06	1.92	0.10
80	0^+–2^+	0.08	0.51	2.41	0.05	0.36	2.77	0 03	1.66	0.09
	4^+–16^+	0.16	0.52	1.92	0.12	0.66	2.35	0.07	2.04	0.11
82	0^+–2^+	0.06	0.54	2.44	0.03	0.30	2.80	0.02	1.68	0.09
	4^+–16^+	0 15	0.51	1.95	0.11	0.63	2.36	0.07	2.08	0.10

Table 4. The sub-shell occupation numbers (neutrons) in the nuclei $^{74\text{-}82}$Kr

Kr nuclei (A)	Sub-shell occupation number								
	J^π	$3s_{1/2}$	$2p_{1/2}$	$2p_{3/2}$	$2d_{3/2}$	$2d_{5/2}$	$1f_{5/2}$	$1g_{7/2}$	$1g_{9/2}$	$1h_{11/2}$
74	0^+–10^+	0 08	0.60	2 61	0.05	0.49	3.27	0.04	2.75	0.08
	12^+–16^+	0.11	0.05	2.31	0.07	0.64	3.15	0.05	3.02	0.07
76	0^+–2^+	0.08	0.83	3.30	0.05	0.50	3.95	0.04	3.22	–0.02
	4^+–16^+	0.17	0.70	3.03	0.15	0.76	3.67	0.11	3.34	0.02
78	0^+–2^+	0.09	1.23	3.66	0.06	0.53	4.73	0.05	3.64	–0.02
	4^+–16^+	0.20	1.01	3.44	0.22	0.77	4.30	0.15	3.88	–0.01
80	0^+–2^+	0.09	1.70	3.86	0.06	0 51	5.50	0.05	4.23	–0.03
	4^+–16^+	0.31	1.52	3.59	0.41	0.85	4.37	0.27	4.52	0.02
82	0^+–2^+	0.08	1 94	3.95	0.06	0.48	5.89	0.04	5.51	0.01
	4^+–16^+	0.36	1.63	3.79	0.49	0.86	5.37	0.31	5.13	0.008

occupation reveals that $\langle Q^2_0 \rangle$ for $^{74\text{-}82}$Kr arises due to significant proton occupation of $2p_{3/2}$, $1f_{5/2}$ and $1g_{9/2}$ proton orbits. The higher lying valence orbits have nearly insignificant proton occupation. An inspection of neutron occupation numbers reveals that out of the higher valence orbits above ($1g_{9/2}$) orbit, only ($2d_{5/2}$) orbit receives about 0.5 neutrons. It is therefore, important to include ($2d_{5/2}$) orbit in the valence space and other higher lying valence orbits can be dropped.

4. Conclusions

From the results of our calculations, the following conclusions can be drawn :

i) The results of VAP calculations show a marked improvement in agreement with experiment over the PHB calculations using PQH interaction.

ii) The hexadecapole interaction parameters employed by us are the appropriate ones for this mass-region and produce accurate HB wave functions which yield values of $B(E2)$ and β_2 in satisfactory agreement with experiment.

iii) The VAP calculations performed with PQH interaction reproduces correctly the deformation systematics in $^{74\text{-}82}$Kr isotopes.

iv) The yrast spectra in $^{76\text{-}82}$Kr isotopes arise from two intrinsic states. The 0^+ and 2^+ states arise from an intrinsic state with smaller quadrupole moments than the higher angular momentum states.

References

[1] M Sakai *At Data and Nucl. Data Tables* **31** 407 (1984)

[2] R B Piercey, A C Rester, J H Hamilton, A V Ramayya H K Carter, J C Wells and J Lin *Phys Rev.* **C32** 625 (1985)

[3] H Sun, J Doring, G D Johns, R A Kaye, G Z Solomon, S L Tabor, M Devlin, D R La Fosse, F Lerma, D G Sarantites, C Baktash, D Rudolph, C H Yu, A O Macchiavelli, I Birrel, J X Saladin, D F Winchell, V Q Wood and I Ragnarsson *Phys Rev* **C59** 655 (1999)

[4] G Mukhejee, H C Jain, R Palit, P K Joshi, S D Paul and S Nagaraj *Phys. Rev.* **C64** 034316-1 (2001)

[5] S Raman, C W Nestor (Jr) and P Tikkanen *At Data and Nucl. Data Tables* **78** 1 (2001)

[6] S Raman, C H Malarkey, W T Milner, C W (Jr.) Nestor and P H Stelson *At. Data Nucl Data Tables* **36** 20 (1987)

[7] J Doring, G D Johns, R A Kaye, M A Riley, S L Tabor and J X Saladin *Phys Lett.* **B381** 40 (1996)

[8] P K Joshi, H C Jain, R Palit, G Mukherjee and S Nagaraj *Nucl. Phys.* **A700** 59 (2002)

[9] C Chandler, P H Regan, C J Pearson, B Blank, A M Bruce, W N Catford, N Curtis, S Czajkowski, W Gelletly, R Grzywacz, Z Janas, M Lewitowicz, C Marchand, N A Orr, R D Page, A Petrovici, A I Reed, M G Saint-Laurent, S M Vincent, R Wadsworth, D D Warner and J S Winfield *Phys Rev* **C56** R2924 (1997)

[10] J Billowes, F Cristancho, H Grawe, C J Gross, J Heese, A W Mountford and M Weiszflog *Phys Rev* **C47** R917 (1993)

[11] A Giannatiempo A Nanni, M J G Borge and K Riisager *Phys Rev* **C47** 521 (1993)

[12] J Heese, D J Blumenthal, A A Chishti, P Chodhury, B Crowell, P J Ennis, C J Lister and Ch Winter *Phys Rev* **C43** R921(1991)

[13] C R Praharaj *J Phys* **G14** 843 (1988)

[14] W Nazarewicz, J Duke, R Bengtsson, I Bengtsson and I Ragnarsson *Nucl Phys* **A435** 397 (1985)

[15] P Moller and J R Nix *1986 Los Alamos National Laboratory Preprint La-UR-86-3983*

[16] P Bonche, H Flocard, P H Heenen, S J Krieger and M S Weiss *Nucl. Phys* **A443** 39 (1985)

[17] X Campi and M Epherre *Phys Rev* **C22** 2605 (1980)

[18] J P Maharana, L S Warrier and Y K Gambhir *Ann Phys* **250** 237 (1996)

[19] K C Tripathy and R Sahu *Nucl Phys* **A597** 177 (1996)

[20] P Sarriguren, E Moya de Guerra and A Escuderos *Nucl Phys* **A658** 13 (1999)

[21] A Petrovici, K W Schmid and A Faessler *Nucl Phys* **A665** 333 (2000)

[22] A Giannatiempo, P Sona and A Nannini *Phys Rev* **C62** 044302 (2000)

[23] C J Gross, J Heese, K P Lieb, S Ulbig, W Nazarewicz, C J Lister, B J Varley, J Billowes, A A Chishti, J H Mc-Neill and W Gelletly *Nucl Phys* **A501** 367 (1989)

[24] R Palit, J A Sheikh, Y Sun and H C Jain *Nucl Phys* **A686** 141 (2001)

[25] R Soundranayagam, S Ramavataram, A V Ramayya, J H Hamilton and R L Robinson *Phys Rev* **C25** 2983 (1982)

[26] S K Khosa and S K Sharma *Phys Rev* **C25** 2715 (1981)

[27] J D Vergados and T T S Kuo *Phys. Lett* **B35** 93 (1971)

[28] S K Sharma, P N Tripathi and S K Khosa *Phys. Rev* **C38** 2935 (1988)

[29] A Bohr and B R Mottelson *Nuclear Structure* (Benjamin : New York) (1975) **Vol II** p 356

[30] S K Sharma *Nucl Phys.* **A260** 226 (1976)

[31] K H Bhatt, C W Nestor (Jr) and S Raman *Phys Rev.* **C46** 164 (1992)

[32] S Raman, C W Nestor (Jr), S Kahane and K H Bhatt *At Data Nucl Data Tables* **42** 1 (1989)

[33] S Raman, J A Sheikh and K H Bhatt *Phys Rev* **C52** 1380 (1995)